Polymer 50 (2009) 898–904

Contents lists available at ScienceDirect

Polymer

journal homepage: www.elsevier.com/locate/polymer

Magnetic field alignment and electrical properties of solution cast PET–carbon nanotube composite films

Brian W. Steinert, Derrick R. Dean*

University of Alabama at Birmingham, Department of Materials Science and Engineering, 1530 3rd Avenue South, Birmingham, AL 35294-4461, USA

ARTICLE INFO

Article history:
Received 17 September 2008
Received in revised form
19 November 2008
Accepted 22 November 2008
Available online 10 December 2008

Keywords:
Carbon nanotube
Magnetic alignment
Electrical conductivity

ABSTRACT

Single-wall carbon nanotubes (SWNTs) were dispersed in a polyethylene terephthalate (PET) matrix by solution blending and then cast onto a glass substrate to create flexible films. Various SWNT loading concentrations were implemented (0.5, 1.0, and 3.0 wt%), and the processing method was repeated to produce films in the presence of magnetic fields (3.0 and 9.4 T). Alignment of the SWNTs in the PET matrix was characterized by Raman spectroscopy. Impedance spectroscopy was utilized to study the electrical behavior of the nanocomposites. It was concluded that SWNT concentration and dispersion are the key variables for improving electrical conductivity, while alignment plays a secondary role. Interestingly, it appears that a magnetic field may prove to be a novel method for improving the dispersion of unmodified SWNTs by disrupting van der Waals interactions.

1. Introduction

Carbon nanotubes (CNTs) have come to the forefront of nanostructured materials research in the past decade, and interest has grown exponentially since the discovery and characterization of CNTs in 1991 [1]. This incredible growth and excitement in CNT research are almost solely due to their excellent, inherent properties and physical parameters. Extensive work has been done to characterize CNTs, including their exceptional mechanical [2–5], thermal [6–9] and electrical characteristics [10–14]. CNTs have also been shown to have extremely high aspect ratios (length/diameter), with diameters of one to tens of nanometers and lengths up to the micrometer, or even centimeter, scale [14,15]. These features make CNTs highly useful in a wide range of potential applications, such as reinforcement nanofillers, probes, energy storage, and various electronic or thermal devices.

Polymer nanocomposites with CNT fillers have been around almost as long as CNTs themselves, with Ajayan et al. publishing the first report on this topic in 1994 [16]. The interest in this area stems from the fact that polymers offer many desirable qualities, such as toughness, space savings, low weight, good surface finish, flexibility, and low cost. Using CNTs as a property enhancing nanofiller for a high performance, lightweight composite is one of the lynchpins of nanocomposite research. The exceptional and unique properties of CNTs offer a great advantage for the production of improved composites, but their utilization within a matrix depends primarily on relationships between the matrix and nanoconstituent; specifically the particle's spatial orientation and interactions at the particle interface.

CNTs have been shown to be a practical polymer reinforcement material for lightweight structural materials by significantly enhancing the toughness, tensile strength, and modulus of a polymer nanocomposite [17–24]. Also, the extreme thermal stability and thermal conductivity that CNTs have exhibited make polymer nanocomposites equally as viable for many thermal management applications, including as packaging and coatings [6–8,23–25]. At the same time, the electrical behavior of CNTs has been one of the most highly studied areas in all of CNT research. Theoretical calculations have shown that the electrical properties of CNTs are very dependent upon their structure, or their rolled configuration (i.e. armchair, zig-zag, or chiral) and diameter, more specifically [10,26]. The nanoscale dimensions, one-dimensional structure, and tubular symmetry of CNTs produce amazing quantum transport effects. Studies have shown that individual CNTs can behave electrically as a single molecule and be defined as quantum wires [13,27]. Very high conductive capability (resistivity, $R = 10^{-8}\,\Omega\,\mathrm{cm}$) has been reported [11,14,28]. This is greater than iron or copper ($R = 10^{-6}\,\Omega\,\mathrm{cm}$) [29], as well as crystalline graphite ($R = 10^{-5}\,\Omega\,\mathrm{cm}$) [30].

CNTs are also naturally highly anisotropic because of their high aspect ratios and strong carbon–carbon bonds parallel to the fiber axis. Therefore, it is critical to take advantage of these facts by

* Corresponding author. Tel.: +1 205 975 4666; fax: +1 205 934 8485.
E-mail address: deand@uab.edu (D.R. Dean).

0032-3861/$ – see front matter © 2008 Elsevier Ltd. All rights reserved.
doi:10.1016/j.polymer.2008.11.053

manipulating the nanoscale particle and imparting anisotropy into the system to produce the highest-performance nanocomposites. Numerous alignment techniques have been attempted to produce this effect, including fiber spinning with drawing [31] and/or with a rotating collector [32], shearing [33,34], plasma-enhanced deposition [35–37], and electric field-induced alignment [38,39]. Another technique that has gained recent attention is magnetic alignment [40–43].

CNTs have been shown to be highly susceptible to a magnetic field [44–50]. Magnetic susceptibility (χ) is the degree of magnetization of a material in response to an applied magnetic field, and it has been the subject of multiple theoretical predictions with respect to CNTs [45,50]. It was found that χ has an increasing, linear dependence on CNT diameter. Also, it has been determined that the χ is dependent on magnetic field direction and temperature. The dependence on magnetic field direction imparts magnetic anisotropy, and therefore CNTs can align in the presence of a magnetic field [50].

With respect to resin, or matrix, material selection, polyethylene terephthalate (PET) is one of the most extensively used thermoplastic polyesters out on the market, and it has been implemented in many forms, including as fibers, films, and moldings. It has been shown to have good thermal stability, strong wear and chemical resistance, and low permeability; which make it extremely attractive for numerous industrial applications. There has been limited work in the area of PET–CNT nanocomposites [51–56], with the majority of all PET related research focused on melt processed properties and morphology. Thus far, work in the area of solution cast PET–SWNT nanocomposites is relatively absent, while other solution cast polymer–CNT systems have been studied [57–59]. This lack of attention makes solution cast PET nanocomposites particularly interesting. Solution casting offers various advantages as a method for producing films, such as less need for a thermal stabilizer and larger production equipment (extruder), which reduces processing costs. Solution casting is also a factor in the roll-to-roll processing technique often utilized for large-scale manufacturing of printable, flexible electronic devices, such as circuits and solar cells [60,61].

The objective of this work was to produce an efficient conductive polymer by studying the effect of single-wall carbon nanotube (SWNT) inclusion and alignment on the electrical conductivity behavior of solution cast polymer nanocomposite films. The relevance of conductive polymers for antistatic or electrostatic dissipation applications is rapidly growing in the marketplace, and this type of research has become increasingly valuable [62]. Previous research in the area of CNT alignment and electrical properties has produced promising results [40,41,43].

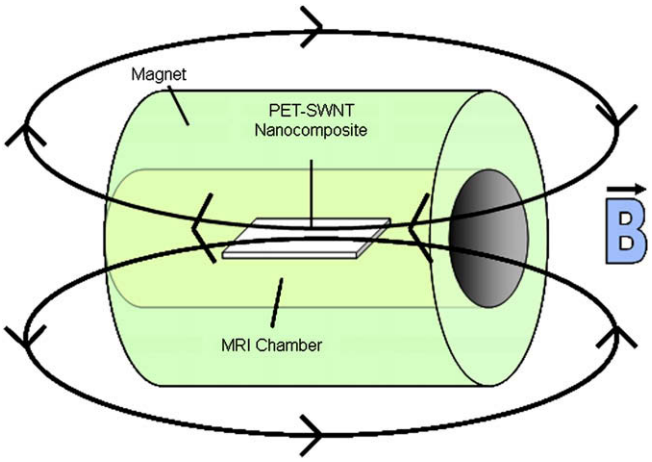

Fig. 2. MRI schematic displaying the placement of the samples with respect to the instrument and subsequent magnetic field ($\vec{B}$).

2. Experimental

2.1. Materials

PET flakes were purchased from Scientific Polymer Products, Inc. (Ontario, NY), while HiPco processed SWNTs were acquired from Rice University. 1,1,1,3,3,3-Hexafluoro-2-propanol (≥99%) (HFP) was purchased from Sigma–Aldrich Co. (St. Louis, MO) to be used as a solvent for the PET polymer.

2.2. Film preparation

2.2.1. Randomly-oriented films

Polymer and nanocomposite thin films (thickness, $t \sim 160$ μm) were created using a simple solution blending and casting technique. For the nanocomposite samples, SWNTs were dispersed in HFP with a Cole–Parmer 8892 ultrasonic bath (frequency, $\upsilon = 42$ kHz) for 4 h to assure the dispersion of large SWNT aggregations throughout the solvent. PET flakes (1:10 PET/HFP) were placed in the HFP–SWNT solution over heat (~75 °C) and continuously mixed with a magnetic stir bar until it appeared that the PET was dissolved in the solution. This was indicated by a visual lack of flakes and an increase in solution viscosity. Solution casting was completed by pouring the solution on top of a glass substrate under a fume hood. A square-shaped polydimethylsiloxane (PDMS) barrier (height, $h = 859$ μm) was used to contain and shape the solution and subsequent film. A doctor's blade was used to level the

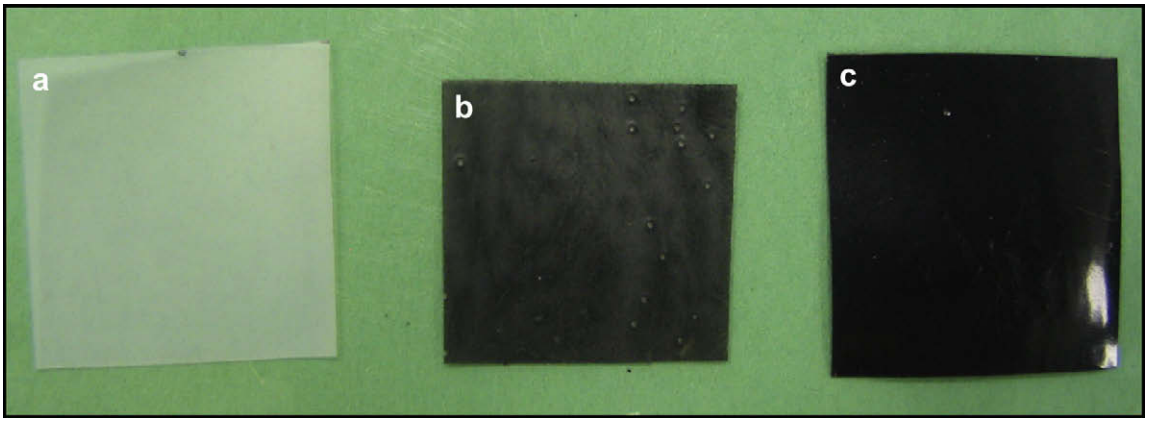

Fig. 1. Digital image of solution cast PET films of varying SWNT loadings (a) 0.0 wt% SWNT, (b) 0.5 wt% SWNT, and (c) 1.0 wt% SWNT.

solution to the barrier height. One large film (area, $A = 400\ cm^2$) of each sample type was produced. Once the solvent had evaporated and crystallization was completed, the film was placed in a Curtin Matheson Scientific, Inc. Equatherm vacuum oven at approximately 90 °C to assist in the removal of any residual solvent in the film. Fig. 1 shows a digital image of various PET films which were solution cast with SWNT loadings of 0.0, 0.5, and 1.0 wt%.

2.2.2. Magnetically aligned films

The aligned films were produced in the same manner as the unaligned films, except after the PET–SWNT solutions were poured onto a glass substrate they were subsequently placed in a large magnetic resonance imaging (MRI) scanner. Two separate MRI scanners were used, each producing different magnetic field strengths. A Siemens Magnetom Allegra was used to produce a 3 T magnetic field, while a Bruker BioSpec® was used to produce a 9.4 T magnetic field. Fig. 2 presents the experimental setup.

2.3. Magnetic alignment characterization

2.3.1. Raman spectroscopy

Raman spectroscopy was performed with a Renishaw inVia microRaman microscope using a 785 nm excitation wavelength, a power of 0.1 mW, a 50× objective lens, a 20 s accumulation time, and 3 accumulations per direction per sample. Raman spectra were obtained for each magnetically aligned nanocomposite sample (0.5, 1.0, and 3.0 wt% SWNT). The tangential mode, or G-peaks ($\sim 1590\ cm^{-1}$), of these spectra was used to analyze the degree of SWNT orientation in the films. Each sample was measured at different angles with respect to the direction of the magnetic field, with 0° corresponding to a direction parallel to the magnetic field and 90° being perpendicular to the field.

2.3.2. Transmission electron microscopy (TEM)

TEM micrographs were acquired with an FEI Tecnai™ G^2 Spirit microscope using an accelerating voltage of 100 kV. Each nanocomposite film was microtomed prior to imaging, parallel and perpendicular to the largest surface area plane, and micrographs were acquired at various magnifications. TEM was used to gather a qualitative understanding of the SWNT alignment.

2.4. Impedance spectroscopy

The AC electrical impedance of the PET–SWNT nanocomposites was measured with a Hewlett Packard 4284A Precision LCR Meter at room temperature. Measurements were acquired across a frequency range of 20 Hz–10^6 Hz. Each aligned sample was measured parallel to the direction of the magnetic field that was placed upon it during processing.

3. Results and discussion

3.1. Magnetic alignment

Due to their magnetic susceptibility [44–50], it should be possible to place SWNTs in a magnetic field and align them in a common orientation parallel to the field direction. Raman spectroscopy is a vital tool when attempting to characterize the degree of alignment of SWNTs in a polymer matrix. A characteristic feature of SWNT spectra can be found at around $1590\ cm^{-1}$. This peak is commonly referred to as the tangential mode (TM), or G-peak, and is attributed to elongations of the carbon–carbon bonds along the longitudinal axis of the CNT. Therefore, if the CNTs are aligned, there should be an increase in the G-peak intensity when they are parallel to the polarized laser excitation plane.

Fig. 3 presents the G-peaks of a representative example of an unaligned film. Each peak is identical and independent of the measurement angle, which illustrates the isotropic nature of the CNTs within the nanocomposite. Fig. 4 shows the G-peak intensities for 0.5, 1.0, and 3.0 wt% SWNT samples processed under a 3 T and 9.4 T magnetic field at varying orientation angles (0° is parallel to the magnetic field and 90° is perpendicular to the magnetic field). Samples with varying SWNT concentrations were prepared in order to gain a better understanding of the effect that SWNT density has on orientation.

The spectra present some very interesting results about the effect of magnetic field strength and SWNT concentration on orientation. Both seem to play a very important role in completing SWNT alignment. An ideal case (perfect alignment along the direction of the magnetic field for 100% of the SWNTs) would produce a G-peak that is very intense parallel to the magnetic field (0°), and diminishes for every other orientation.

The G-peak intensity results suggest incomplete alignment for all three SWNT concentrations processed with a 3 T magnetic field, with the primary orientation being approximately 30° off-parallel. Also, the peak spacing between each orientation (0°–90°) gives a good visual representation of the anisotropy of the SWNTs in the PET matrix. As the SWNT concentration increases, the effect of the magnetic field is diminished further and a decrease in the peak spacing is observed. This corresponds to a more isotropic behavior, and it is most likely caused by increasing restrictions on SWNT mobility due to an increase in solution viscosity and nanotube bundling/interactions. Alignment with a much stronger magnetic field (9.4 T) supports this idea. The 9.4 T magnetic field is able to overcome the obstacles that inhibited complete alignment at a low SWNT concentration (0.5 wt%), while the more isotropic behavior at higher concentrations is less prominent. The Raman peak spacings are larger for the 9.4 T processed samples as compared to their 3 T counterparts, which means the higher field strength is able to produce more aligned samples at higher SWNT concentrations. This is corroborated by TEM micrographs (Fig. 5), which show the effect of varying the magnetic field strength on SWNT orientation.

The micrographs present a qualitative measurement of the effect of magnetic field strength on SWNT alignment within a PET matrix. The 3.0 wt% SWNT sample processed at 3 T (Fig. 5a) shows slight, generalized alignment of the SWNTs while a large quantity

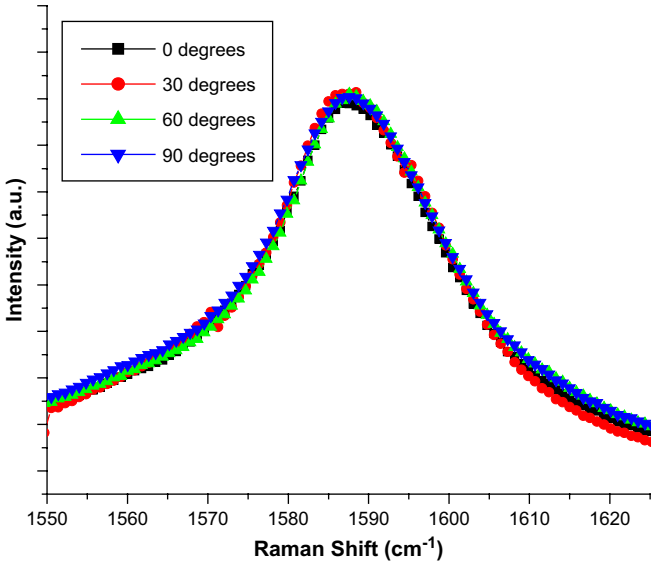

Fig. 3. G-peak spectra of an unaligned PET–SWNT nanocomposite film showing the independence of the measurement angle relative to the orientation of the SWNTs.

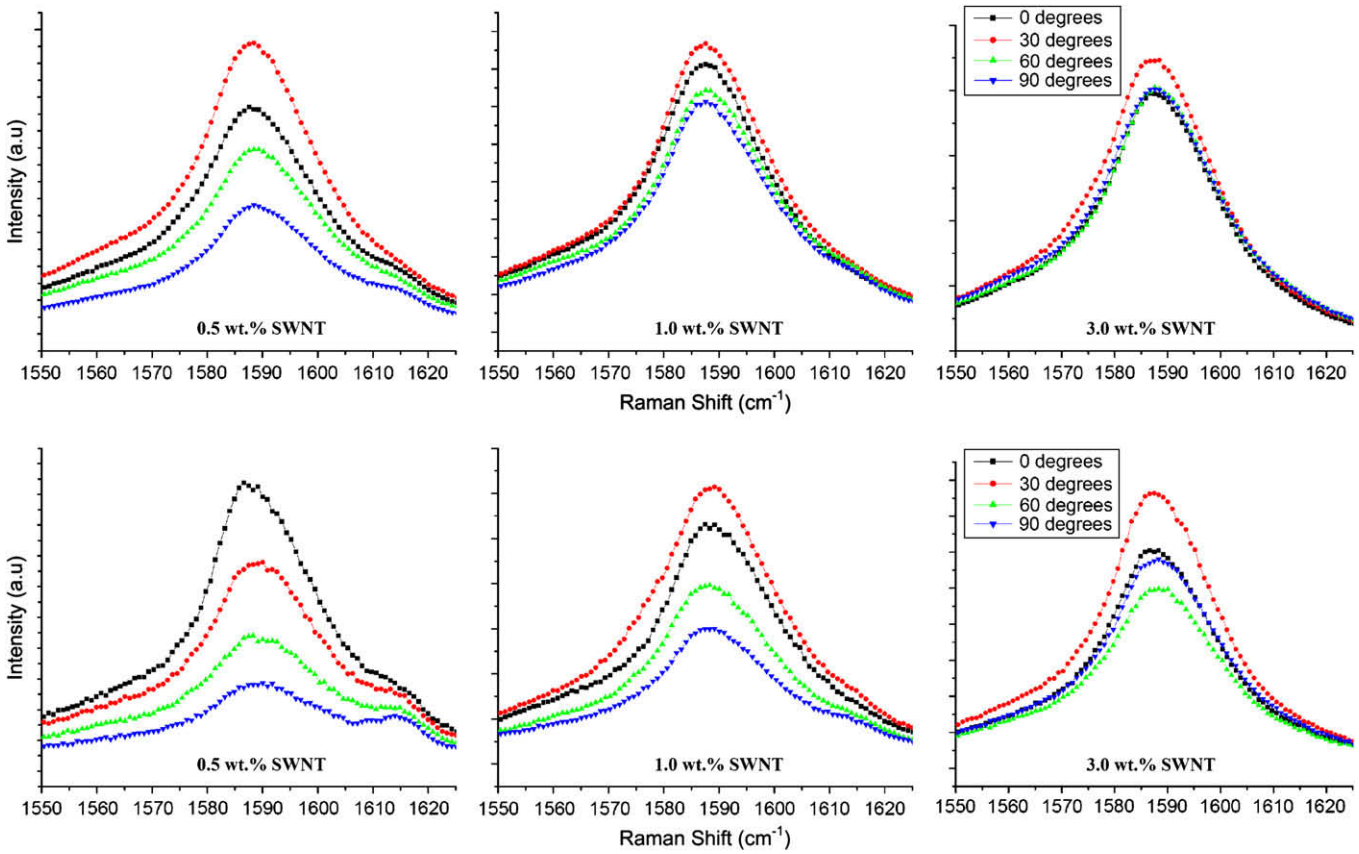

Fig. 4. G-peak intensities relative to the magnetic field direction (0° = parallel) of Raman spectra for samples with varying SWNT loadings and magnetic field processing parameters.

of the nanotubes are unextended. Due to the manner in which many of the SWNTs in the micrograph appear bent but directed towards the direction of the magnetic field, it would seem to indicate that the SWNTs were in the process of aligning to the field but were not able to completely extend before solidification impeded their motion. The 9.4 magnetic field was strong enough to achieve much better SWNT alignment (Fig. 5b), in the allotted processing time. This implies that an adjusted solution-based sample preparation process with slower solvent evaporation may yield aligned SWNTs in a 3 T magnetic field.

Therefore, it appears that magnetic alignment may be a practical technique for establishing anisotropy in a nanocomposite system. It can partially occur under magnetic field strengths as low as 3 T, with the SWNT concentration and magnetic field strength playing important roles in determining the degree of orientation. Though a 3 T magnetic field was not able to achieve complete alignment,

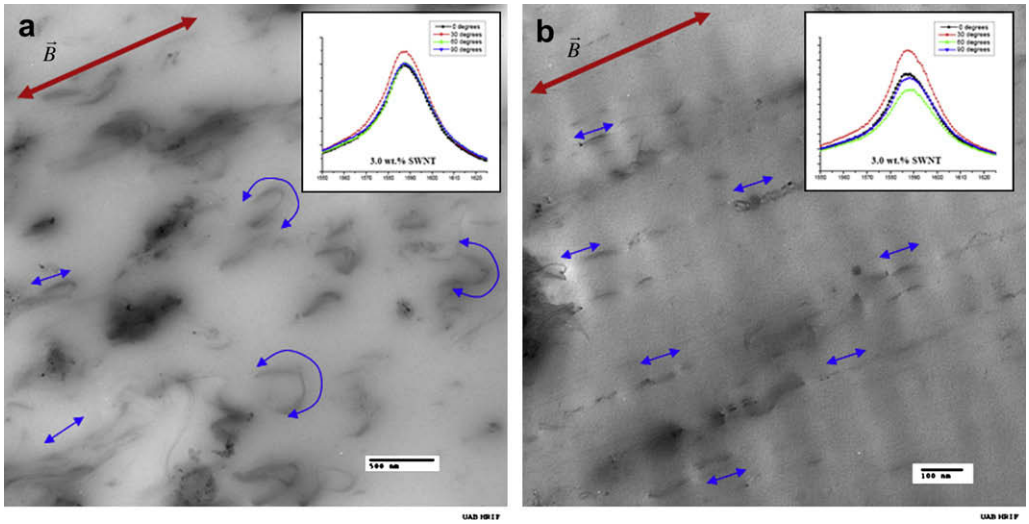

Fig. 5. TEM micrographs showing the effect of magnetic field strength at a constant SWNT loading (3.0 wt%), but with varying magnetic field strengths of (a) 3.0 T and (b) 9.4 T. Corresponding Raman spectra scans from Fig. 4 are insets.

even at low SWNT loadings, the samples processed at this parameter may still prove to be a very effective conductive material. It has been reported that complete alignment may not be ideal for enhancing conductivity, due to an increase in void space between nanotubes [63,64]. Straight lines of SWNTs do not agree with the model of an interconnecting network that produces percolation. Improving SWNT behavior by taking advantage of their anisotropic nature while reducing void space and nanotube-to-nanotube distance with only slight alignment (30° off-parallel) could potentially produce the best electrically conductive behavior [33,65].

3.2. Electrical conductivity

From the impedance spectroscopy data, the electrical conductivity as a function of frequency can be determined (Fig. 6). By plotting conductivity as a function of SWNT concentration, the relative percolation threshold of each sample type was estimated (Fig. 7). Fig. 7 shows the electrical conductivities at 60 Hz as a function of SWNT mass fraction and dependent upon magnetic field strength. Based on the conductivity of pure PET material, the addition of 0.5 and 1.0 wt% SWNTs approximately produced a 7 order of magnitude increase, while the addition of 3.0 wt% SWNTs in a 3 and 9.4 T magnetic field produced an 8 and 9 order of magnitude increase, respectively. Therefore, it can be assumed that the percolation threshold is approximately 0.5 wt% SWNT. This value agrees satisfactorily with previous values observed in other polymer–CNT nanocomposite studies [53,56,63,66–69].

Also shown in Fig. 7 are the relative applications for these materials based on their conductive behaviors. It is noticeable that at 0.5 wt% SWNT, the conductivity of the samples exceeds the antistatic and electrostatic dissipation conditions, but electromagnetic interference (EMI) shielding ($\sim 10^{-4}$ S cm^{-1}) would not be possible.

From the results, it was observed that when SWNT concentration reaches 3.0 wt% there is an increase in electrical conductivity and non-dielectric behavior. The simple explanation to describe this behavior is to associate it with the increase in filler concentration and conclude that more filler material produces a more extensive electron flow network. However, a similar increase is not observed when the SWNT concentration reaches 0.5 and 1.0 wt% for the unaligned or aligned samples, and so there must be

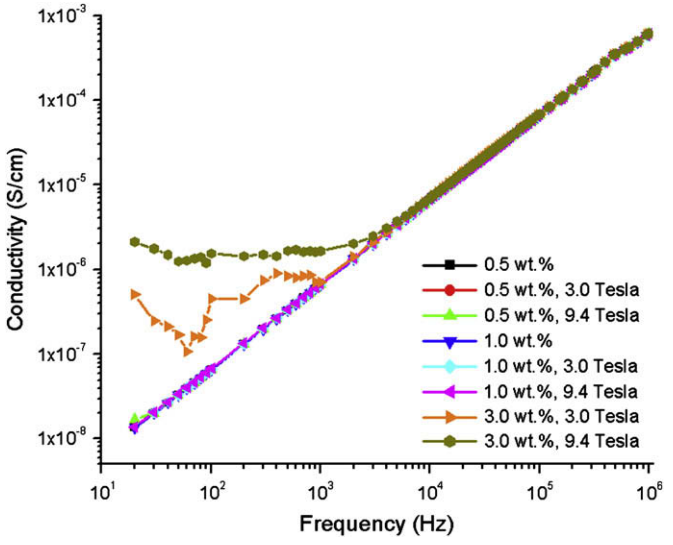

Fig. 6. Log–log plot of the AC conductivity as a function of frequency for various nanocomposite samples.

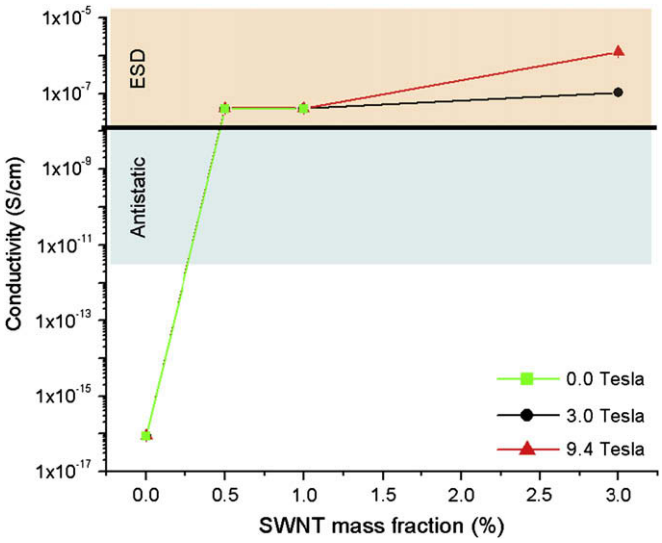

Fig. 7. Log (AC conductivity) as a function of SWNT mass fraction at 60 Hz showing dependence on magnetic field strength, and the relative applications based on the values.

supplementary details that require rationalization. Also, the explanation cannot be directly connected to the creation of a percolation network at 3.0 wt%, because as previously stated, a percolation threshold was achieved at approximately 0.5 wt%.

The frequency dependent behavior observed at 0.5 and 1.0 wt% implies the existence of large gap distances between conductive particles within the matrix, and thus the formation of aggregated SWNT domains. This is synonymous with relatively poor dispersion. This behavior is not unusual for SWNTs, because SWNTs express fairly strong self-attraction due to van der Waals forces between the nanotubes [70,71]. The increase in gap distance between domains results in a buildup of electron flow in the matrix void space. Percolation is ideal, and conductivity is maximized, when physical contact exists between the CNTs, but that situation is not absolutely necessary since current may be able to cross small voids to flow across a device [72], which has presumably occurred in the 0.5 and 1.0 wt% neat samples.

When the SWNT concentration is 3.0 wt% and manipulated with a magnetic field, there is a dramatic change in the electrical behavior at low frequencies. As mentioned, the change cannot be attributed solely to filler concentration. This suggests that the magnetic fields must be invoking an effect. If the SWNTs have a tendency to aggregate, then something must be inhibiting this aggregation to some extent in the aligned 3.0 wt% samples, because they display a frequency-independent, non-dielectric region at low frequencies (Fig. 6). This behavior is more prominent (wider non-dielectric range, greater conductivity) for the 9.4 T processed sample than for the 3 T processed sample. The increased conductivity and non-dielectric range in the 9.4 T sample suggests that the sample has better dispersion. A more dispersed sample possesses smaller gaps between conductive particles, which means more electrons can easily 'hop' between particles and flow across a device.

How is the improved dispersion and greater electrical conductivity at higher concentrations of the aligned samples explained? It cannot be solely due to improved alignment, because it has been concluded in the previous section (3.1) that ideal alignment occurs at a low filler concentration and a high magnetic field strength. According to the Raman spectra (Fig. 4), the 3.0 wt% sample processed at 3 T is basically isotropic with respect to the SWNTs. The 9.4 T processed sample has slightly better alignment according to

the respective spectra. Also, there is almost no difference in the electrical behavior between the aligned SWNTs processed at each magnetic field strength of the 0.5 and 1.0 wt% samples. If the improved results had a direct correlation with alignment, then the same improvement observed at 3.0 wt% should be observed at lower concentrations, especially since there is much greater disparity in the degree of alignment when comparing the effect of field strength at lower concentrations.

Therefore, if the explanation cannot be attributed to concentration or alignment alone, then the answer may be a combination of these effects. The ability to flow into aggregated domains appears to be a problem for samples with lower concentration (0.5 and 1.0 wt%), because there is plenty of void space between SWNTs and their motion is therefore not significantly inhibited. This same effect was observed and discussed in the G-peak analysis of the Raman spectra to describe the alignment behavior. This may also help to explain the dispersion and conductivity improvement shown in the 3.0 wt% samples. As shown in Fig. 4, the SWNTs were not able to completely align and overcome the resistive forces that arise with increased tube-to-tube interaction and solution viscosity. If this interaction can inhibit motion in one plane, then why it cannot have the same effect in all others? The 3.0 wt% SWNT samples appear to exceed a 'density threshold', where the tendency to flow into aggregated domains is counteracted by the lack of void space and freedom to do so. Therefore, the SWNTs, for the most part, are forced to remain in a semi-dispersed state, which creates a more conductive network than an aggregated state.

At the same time, the magnetic field is also producing a beneficial effect to the material. The 3.0 wt% sample processed at 3 T is essentially isotropic, and so the electrical improvement observed for this sample can be considered almost identical to the improvement that would be expected from a 3.0 wt% sample not processed with an applied magnetic field. However, a 9.4 T field is strong enough to invoke an effect, which could be explained with either of the following scenarios, or a combination of the two:

1. The magnetization, or force upon the nanotube, that an SWNT experiences from an applied magnetic field reduces the effect of the van der Waals forces that attract the SWNTs to each other. It has been reported that weakly bound van der Waals complexes can dissociate in a magnetic field through coupling between the Zeeman energy levels [73]. At zero magnetic field strength, van der Waals complexes are stable while an external magnetic field can split Zeeman energy levels, and bound states may be higher in energy. This encourages molecular dissociation, and the dissociation efficiency increases with increasing field strength. Thus, even though there is very little motion due to overcrowding of the SWNTs, any motion that does occur is halted and reduced further. This results in a more dispersed sample, and the increase in the non-dielectric range and conductivity is observed in the results (Figs. 6 and 7).
2. The slight improvement in alignment observed in Fig. 4, when comparing the 3.0 wt% sample processed at 3 T to the 9.4 T sample, creates a better and more anisotropic network, which improves electrical behavior. This same effect is not observed at lower concentrations (despite greater alignment), because the distance between the conductive particles is too great. Most likely, the effect of the magnetic fields is a combination of this scenario with the first scenario.

Overall, it appears that the most important contributing factors to electrical conductivity in a nanocomposite are filler concentration and dispersion. Alignment appears to impart a secondary consequence, as long as a 'density threshold' has been reached. An interesting finding seems to be that a strong enough magnetic field may improve dispersion by disrupting the effect of the van der Waals forces and inhibiting SWNT flow. This could prove to be a very important attribute to consider for future nanocomposite manufacturing, because developing a method to achieve good dispersion of unmodified SWNTs in a polymer could produce unprecedented properties.

4. Conclusions

Solution casting was effectively employed to produce PET–SWNT nanocomposite films, while magnetic fields were used to induce SWNT alignment within the PET matrix. Raman spectroscopy and TEM were utilized to measure the effectiveness of the magnetic fields for aligned SWNTs in a polymer matrix, and it was determined that the field strength and filler concentration play the most important roles in determining the degree of alignment. Low concentration and high magnetic field strength produced the most highly aligned samples. The electrical properties of unaligned and aligned film samples were investigated by impedance spectroscopy, and it was shown that sufficient conductivity for antistatic and electrostatic dissipation purposes can be achieved at concentrations as low as 0.5 wt% SWNT. It was also concluded that dispersion and filler concentration have the greatest effect upon electrical conductivity, while alignment plays a secondary role. However, it was determined that it may be possible to use a magnetic field to improve dispersion, or at least produce a more anisotropic network. This could have important implications in future applications, and it may prove to be a novel method for achieving good dispersion of unmodified SWNTs in polymer matrices.

Acknowledgements

This work was supported by the National Science Foundation (NSF) through the Division of Materials Research (DMR) Grant No. 0404278.

References

[1] Iijima S. Nature 1991;354:56–8.
[2] Treacy MMJ, Ebbesen TW, Gibson JM. Nature 1996;381:678–80.
[3] Krishnan A, Dujardin E, Ebbesen TW, Yianilos PN, Treacy MMJ. Phys Rev B 1998;58:14013–9.
[4] Pan ZW, Xie SS, Lu L, Chang BH, Sun LF, Zhou WY, et al. Appl Phys Lett 1999;74:3152–4.
[5] Natsuki T, Tantrakarn K, Endo M. Appl Phys A Mater Sci Process 2004;79:117–24.
[6] Hone J, Whitney M, Piskoti C, Zettl A. Phys Rev B 1999;59:R2514–6.
[7] Berber S, Kwon Y-K, Tománek D. Phys Rev Lett 2000;84:4613–6.
[8] Che J, agin T, Iii WAG. Nanotechnology 2000;11:65–9.
[9] Motoo F, Xing Z, Huaqing X, Hiroki A, Koji T, Tatsuya I, et al. Phys Rev Lett 2005;95:0655021–4.
[10] Hamada N, Sawada S-i, Oshiyama A. Phys Rev Lett 1992;68:1579–81.
[11] Ebbesen TW, Lezec HJ, Hiura H, Bennett JW, Ghaemi HF, Thio T. Nature 1996;382:54–6.
[12] Langer L, Bayot V, Grivei E, Issi JP, Heremans JP, Olk CH, et al. Phys Rev Lett 1996;76:479–82.
[13] Tans SJ, Devoret MH, Dai H, Thess A, Smalley RE, Geerligs LJ, et al. Nature 1997;386:474–7.
[14] Li S, Yu Z, Rutherglen C, Burke PJ. Nano Lett 2004;4:2003–7.
[15] Zheng LX, O'Connell MJ, Doorn SK, Liao XZ, Zhao YH, Akhadov EA, et al. Nat Mater 2004;3:673–6.
[16] Ajayan P, Stephan O, Colliex C, Trauth D. Science 1994;265:1212–4.
[17] Andrews R, Weisenberger MC. Curr Opin Solid State Mater Sci 2004;8:31–7.
[18] Coleman JN, Khan U, Gun'ko YK. Adv Mater 2006;18:689–706.
[19] Wu M, Shaw L. J Appl Polym Sci 2006;99:477–88.
[20] Cadek M, Coleman JN, Barron V, Hedicke K, Blau WJ. Appl Phys Lett 2002;81:5123–5.
[21] Safadi B, Andrews R, Grulke EA. J Appl Polym Sci 2002;84:2660–9.
[22] Cadek M, Coleman J, Ryan K, Nicolosi V, Bister G, Fonseca A, et al. Nano Lett 2004;4:353–6.
[23] Breuer O, Sundararaj U. Polym Compos 2004;25:630–45.
[24] Moniruzzaman M, Winey KI. Macromolecules 2006;39:5194–205.

[25] Fei D, Quan-Shui Z, Li-Feng W, Ce-Wen N. Appl Phys Lett 2007;90:021914-1–021914-3.
[26] Mintmire JW, Dunlap BI, White CT. Phys Rev Lett 1992;68:631–4.
[27] Dekker C. Phys Today 1999:22–8.
[28] McEuen PL, Fuhrer MS, Hongkun P. IEEE Trans Nanotechnol 2002;1:78–85.
[29] MatWeb. Automation Creations, Inc.; 2007.
[30] Primak W, Fuchs LH. Phys Rev 1954;95:22–31.
[31] Sennett M, Welsh E, Wright JB, Li WZ, Wen JG, Ren ZF. Appl Phys A Mater Sci Process 2003;76:111–3.
[32] Jose MV, Steinert BW, Thomas V, Dean DR, Abdalla MA, Price G, et al. Polymer 2007;48:1096–104.
[33] Lanticse LJ, Tanabe Y, Matsui K, Kaburagi Y, Suda K, Hoteida M, et al. Carbon 2006;44:3078–86.
[34] Abdalla M, Dean D, Adibempe D, Nyairo E, Robinson P, Thompson G. Polymer 2007;48:5662–70.
[35] Ren ZF, Huang ZP, Xu JW, Wang JH, Bush P, Siegal MP, et al. Science 1998;282:1105–7.
[36] Chris B, Wei Z, Sungho J, Otto Z. Appl Phys Lett 2000;77:830–2.
[37] Huang ZP, Xu JW, Ren ZF, Wang JH, Siegal MP, Provencio PN. Appl Phys Lett 1998;73:3845–7.
[38] Park C, Wilkinson J, Banda S, Ounaies Z, Wise KE, Sauti G, et al. J Polym Sci Part B Polym Phys 2006;44:1751–62.
[39] Martin CA, Sandler JKW, Windle AH, Schwarz MK, Bauhofer W, Schulte K, et al. Polymer 2005;46:877–86.
[40] Kimura T, Ago H, Tobita M, Ohshima S, Kyotani M, Yumura M. Adv Mater 2002;14:1380–3.
[41] Choi ES, Brooks JS, Eaton DL, Al-Haik MS, Hussaini MY, Garmestani H, et al. J Appl Phys 2003;94:6034–9.
[42] Garmestani H, Al-Haik MS, Dahmen K, Tannenbaum R, Li D, Sablin SS, et al. Adv Mater 2003;15:1918–21.
[43] Camponeschi E, Vance R, Al-Haik M, Garmestani H, Tannenbaum R. Carbon 2007;45:2037–46.
[44] Heremans J, Olk CH, Morelli DT. Phys Rev B 1994;49:15122–5.
[45] Lu JP. Phys Rev Lett 1995;74:1123–6.
[46] Smith BW, Benes Z, Luzzi DE, Fischer JE, Walters DA, Casavant MJ, et al. Appl Phys Lett 2000;77:663–5.
[47] Walters DA, Casavant MJ, Qin XC, Huffman CB, Boul PJ, Ericson LM, et al. Chem Phys Lett 2001;338:14–20.
[48] Likodimos V, Glenis S, Guskos N, Lin CL. Phys Rev B 2003;68:045417.
[49] Ajiki H, Ando T. Phys Rev B Condens Matter 1994;201:349–52.
[50] Ajiki H, Ando T. J Phys Soc Jpn 1995;64:4382–91.
[51] Li Z, Luo G, Wei F, Huang Y. Compos Sci Technol 2006;66:1022–9.
[52] Anand KA, Agarwal US, Joseph R. Polymer 2006;47:3976–80.
[53] Hu G, Zhao C, Zhang S, Yang M, Wang Z. Polymer 2006;47:480–8.
[54] Wang Y, Deng J, Wang K, Zhang Q, Fu Q. J Appl Polym Sci 2007;104:3695–701.
[55] Shin DH, Yoon KH, Kwon OH, Min BG, Hwang CI. J Appl Polym Sci 2006;99:900–4.
[56] Anand KA, Agarwal US, Joseph R. J Appl Polym Sci 2007;104:3090–5.
[57] Probst O, Moore EM, Resasco DE, Grady BP. Polymer 2004;45:4437–43.
[58] You J-W, Chiu H-J, Don T-M. Polymer 2003;44:4355–62.
[59] Minus ML, Chae HG, Kumar S. Polymer 2006;47:3705–10.
[60] Makela T, Jussila S, Kosonen H, Backlund TG, Sandberg HGO, Stubb H. Synth Met 2005;153:285–8.
[61] Shinohara H, Abe M, Nishi K, Arai Y. Photovoltaic energy conversion, 1994; 1994.
[62] Conductive polymers. Norwalk, CT: Business Communications Company, Inc.; 2003.
[63] Du F, Fischer JE, Winey KI. J Polym Sci Part B Polym Phys 2003;41:3333–8.
[64] Munson-McGee SH. Phys Rev B 1991;43:3331.
[65] Du F, Fischer JE, Winey KI. Phys Rev B Condens Matter 2005;72:121404.
[66] Sandler JKW, Kirk JE, Kinloch IA, Shaffer MSP, Windle AH. Polymer 2003;44:5893–9.
[67] Chang TE, Kisliuk A, Rhodes SM, Brittain WJ, Sokolov AP. Polymer 2006;47:7740–6.
[68] Antonucci V, Faiella G, Giordano M, Nicolais L, Pepe G. Macromol Symp 2007;247:172–81.
[69] Seo M-K, Park S-J. Chem Phys Lett 2004;395:44–8.
[70] Dresselhaus MS, Dresselhaus G, Avouris P, editors. Carbon nanotubes: synthesis, structure, properties, and applications. New York, NY: Springer; 2001.
[71] Meyyappan M, editor. Carbon nanotubes: science and applications. Boca Raton, FL: CRC Press LLC; 2005.
[72] Curran S, Zhang D, Wondmagegn W, Ellis A, Cech J, Roth S, et al. J Mater Res 2006;21:1071–7.
[73] Krems RV. Phys Rev Lett 2004;93:013201.